The following publication Junwei Zhang, Xiong Wu, Qifeng Yan, Heyun Tan, Xiaojian Hong, Chao Fei, Alan Pak Tao Lau, and Chao Lu, "Nonlinearity-aware PS-PAM-16 transmission for C-band net-300-Gbit/s/λ short-reach optical interconnects with a single DAC," Opt. Lett. 47, 3035-3038 (2022) is available at https://dx.doi.org/10.1364/OL.462013.

Nonlinearity-aware PS-PAM-16 transmission for C-band net-300-Gbit/s/λ short-reach optical interconnects with a single DAC

JUNWEI ZHANG,[1,2,*] XIONG WU,[2] QIFENG YAN,[3] HEYUN TAN,[1,*] XIAOJIAN HONG,[4] CHAO FEI,[4] ALAN PAK TAO LAU,[5,6] AND CHAO LU[2,6]

[1] State Key Laboratory of Optoelectronic Materials and Technologies, School of Electronics and Information Technology, Sun Yat-Sen University, Guangzhou 510006, China
[2] Photonics Research Institute, Department of Electronic and Information Engineering, The Hong Kong Polytechnic University, Hong Kong SAR, China
[3] South China Academy of Advanced Optoelectronics, South China Normal University, Guangzhou 510006, China
[4] Ningbo Research Institute, Zhejiang University, Ningbo 315100, China
[5] Photonics Research Institute, Department of Electrical Engineering, The Hong Kong Polytechnic University, Hong Kong SAR, China
[6] The Hong Kong Polytechnic University Shenzhen Research Institute, Shenzhen 518057, China
**Corresponding author: tanhy35@mail.sysu.edu.cn; zhangjw253@mail.sysu.edu.cn*

Received XX Month XXXX; revised XX Month, XXXX; accepted XX Month XXXX; posted XX Month XXXX (Doc. ID XXXXX); published XX Month XXXX

A nonlinearity-aware signal transmission scheme based on a low-complexity 3rd-order diagonally-pruned absolute-term nonlinear equalizer with weight sharing (DP-AT-NLE-WS) and rate-adaptable probabilistically shaped 16-level pulse amplitude modulation (PS-PAM-16) signal is proposed and experimentally demonstrated for C-band net-300-Gbit/s/λ short-reach optical interconnects. By replacing the multiplication operation with the absolute operation and applying weight sharing to reduce the kernel redundancy, the computational complexity of the proposed 3rd-order DP-AT-NLE-WS is reduced by >40% compared to the 3rd-order DP-Volterra NLE (DP-VNLE), DP-AT-NLE and DP-VNLE-WS, with the achieved normalized general mutual information (NGMI) above the threshold of 0.857. Employing a commercial 32-GHz Mach-Zehnder modulator (MZM) and a single digital-to-analog converter (DAC), we demonstrate the single-lane transmission of 100-GBaud PS-PAM-16 signal using DP-AT-NLE-WS in C-band at record 370-Gbit/s line rate and 300.4-Gbit/s net rate over 1-km standard single-mode fiber (SSMF), achieving 21.2% (15.5%) capacity improvement over 100 (105)-GBaud PAM-8 transmission. To the best of our knowledge, this is the first net-300-Gbit/s intensity modulation and direct detection (IM/DD) short-reach transmission in C-band using commercially available components. © 2022 Optica Publishing Group

With the continuously growing popularity of various bandwidth-hungry applications, such as video streaming, artificial intelligence, cloud computing, augmented reality (AR) and virtual reality (VR), intra-data-center (intra-DC) traffic is facing the great challenges in capacity. Since the intra-DC is particularly sensitive to cost, power consumption and footprint, intensity modulation and direct detection (IM/DD) scheme is preferred compared to coherent detection technology [1, 2]. Among different IM/DD schemes, pulse amplitude modulation (PAM) shows an optimal balance between performance and complexity, thus 400G Ethernet with PAM-4 has already been standardized [3]. For the next-generation Ethernet targeting 800G and 1.6T over short-reach distances, 200-Gbit/s/λ IM/DD link is a promising solution to achieve the best trade-off among cost, size and power [4]. In addition, net-300-Gbit/s/λ PAM solution may be an attractive choice for beyond 1-Tbit/s intra-DC interconnects over 4 lanes.

Recently, short-reach IM/DD transmissions with single-wavelength net data rates ranging from 200 to 250 Gbit/s were demonstrated [5–7] for standard single-mode fiber (SSMF) links with transmission distances up to 2 km using C-band commercial Mach-Zehnder modulators (MZMs) and devices only. In addition to commercial devices, specially-designed and manufactured high-performance components such as high-bandwidth super-digital-to-analog converter (super-DAC) [8], digital band-interleaved (DBI) DAC [9], and combination of DBI DAC and 100-GHz thin-film LiNbO3 Mach-Zehnder modulator (MZM) [10] have been reported to support C-band IM/DD transmissions with single-wavelength net date rates beyond 400 Gbit/s using probabilistically shaped PAM (PS-PAM) and PAM signals. However, the commercial immaturity of emerging integrated devices and complicated system architectures inevitably increase the cost and complexity for short-reach optical interconnects. Therefore, it is worth improving the data rate of short-reach transmission systems further by high-efficiency modulation and equalization with current commercial devices.

In this letter, we propose and experimentally demonstrate a nonlinearity-aware signal transmission scheme based on a low-complexity 3rd-order diagonally-pruned absolute-term nonlinear equalizer with weight sharing (DP-AT-NLE-WS) and rate-adaptable PS-PAM-16 signal for net-300-Gbit/s/λ short-reach optical interconnects in C-band. For DP-AT-NLE-WS, the multiplication operation is replaced with the absolute operation and *k*-means clustering based weight sharing is applied to reduce the kernel redundancy, which results in > 40% reduction in complexity compared with the DP-VNLE, DP-AT-NLE and DP-VNLE-WS with the achieved normalized general mutual information (NGMI) above the soft-decision forward error correction (SD-FEC) threshold of 0.857. Employing a commercial 32-GHz MZM and a single DAC, we successfully realize C-band single-lane 100-GBaud PS-PAM-16 signal transmission using low-complexity DP-AT-NLE-WS at record 370-Gbit/s line rate and 300.4-Gbit/s net rate over 1-km SSMF. Meanwhile, compared with 100 (105)-GBaud PAM-8 signal, the achieved net data rate of 100-GBaud PS-PAM-16 signal is improved by 21.2% (15.5%) at the NGMI threshold of 0.857. The results show that the nonlinearity-aware PS-PAM-16 transmission scheme is a promising solution for short-reach optical interconnects beyond net 300 Gbit/s/λ.

To mitigate the linear and nonlinear distortions of transceiver while maintaining relatively low complexity in short-reach IM/DD transmission, a diagonally-pruned absolute-term nonlinear equalizer called DP-AT-NLE [11] can be implemented as a post-equalizer at the receiver side. Here 3rd-order absolute terms are introduced to further enhance the equalization performance. The output of *n*th sample of the 3rd-order DP-AT-NLE can be expressed as

$$y(n)=\sum_{k=0}^{N_1-1}h_1(k)x(n-k)+\sum_{q=0}^{Q-1}\sum_{k=0}^{N_2-1-q}h_2(k,q)\left|x(n-k)+x(n-k-q)\right|+\sum_{k=0}^{N_3-1}h_3(k)\left|x(n-k)\right|x(n-k) \quad \textbf{(1)}$$

where $x(n)$ is the *n*th sample of the received signal corrupted by linear and nonlinear distortions, h_m and N_m are the *m*th-order (m = 1, 2, 3) kernel and memory length of the DP-AT-NLE, respectively. Q is the pruning factor for 2nd-order operation. To balance the performance and complexity, here only the 3rd-order main diagonal terms are included for 3rd-order operation. It can be seen that the term $x(n)x(n\text{-}q)$ in DP-VNLE is replaced with $|x(n)+x(n\text{-}q)|$ in DP-AT-NLE [11], thus avoiding huge multiplication operations and reducing the computational complexity. The total number of kernels is $L = N_1+Q(2N_2\text{-}Q+1)/2+N_3$. The kernels of DP-AT-NLE can be estimated via training sequence before data transmission.

To further lower the computational complexity, *k*-means clustering is performed for L estimated kernels (i.e, h_1, h_2, and h_3) of DP-AT-NLE and the resulted cluster centroids are served as new kernels for nonlinear equalization [12] with the proposed 3rd-order DP-AT-NLE-WS, which is given by

$$y_c(n)=\sum_{i=0}^{N_c-1}w(i)x_c(n,i) \quad \textbf{(2)}$$

where $w(i)$ and N_c are centroid (i.e., new kernel) and the number of clusters obtained by the *k*-means clustering algorithm [12], respectively. $x_c(n, i)$ is the sum of the corresponding linear and nonlinear terms (i.e., $x(n\text{-}k)$, $|x(n\text{-}k) + x(n\text{-}k\text{-}q)|$, and $|x(n\text{-}k)|x(n\text{-}k)$) with their kernels belonging to the *i*th cluster with a centroid of $w(i)$. After clustering, the number of weight-sharing kernels is reduced from L to N_c.

The computational complexity of the proposed 3rd-order DP-AT-NLE-WS, which is evaluated by the required number of real-valued multiplications (RNRM) in one PAM symbol, is compared with that of 3rd-order DP-VNLE, DP-AT-NLE and DP-VNLE-WS. The results are presented in Table 1. The proposed 3rd-order DP-AT-NLE-WS only needs N_3 and N_c real-valued multiplications to calculate $|x(n\text{-}k)|x(n\text{-}k)$ and perform weight-sharing equalization as presented in Eq. (2), respectively. As comparisons, 3rd-order DP-VNLE and DP-AT-NLE require $N_1+Q(2N_2\text{-}Q+1)+3N_3$ and $N_1+Q(2N_2\text{-}Q+1)/2+2N_3$ real-valued multiplications [11], respectively. With respect to 3rd-order DP-VNLE-WS, $Q(2N_2\text{-}Q+1)/2$ and $2N_3$ real-valued multiplications are required to obtain 2nd- and 3rd-order terms respectively, before performing weight-sharing equalization.

Table 1. Complexity comparison of different 3rd-order NLEs.

Equalizer	RNRM of *m*th-order operation		
	1st-order	2nd-order	3rd-order
DP-VNLE [11]	N_1	$Q(2N_2\text{-}Q+1)$	$3N_3$
DP-AT-NLE [11]	N_1	$Q(2N_2\text{-}Q+1)/2$	$2N_3$
DP-VNLE-WS	$N_c+Q(2N_2\text{-}Q+1)/2+2N_3$		
DP-AT-NLE-WS	N_c+N_3		

The performance of the proposed nonlinearity-aware signal transmission scheme based on DP-AT-NLE-WS and rate-adaptable PS-PAM-16 is evaluated in a short-reach transmission system as the experimental setup and digital signal processing (DSP) block diagram shown in Fig. 1. For PS-PAM-16 signal generation, Maxwell-Boltzmann (MB) distribution using constant composition distribution matcher (CCDM) with a symbol block length of 2^{12} is applied [8]. Inset (a) presents the probability distribution of PS-PAM-16 signal with 3.7 bits/symbol. The generated PS-PAM-16 signal is up-sampled and pulse shaped by a raised-cosine (RC) filter with a roll-off factor of 0.01. Then the resulted PS-PAM-16 signal is resampled and fed into an arbitrary waveform generator (AWG, Keysight M8194A) at 120 GSa/s to generate 100-GBaud electrical signal. After that, the PS-PAM-16 signal is amplified by an electrical amplifier (EA, SHF 807) before driving a 32-GHz MZM (FTM 7938EZ) operating at a quadrature point of around 4.2 V. The optical carrier is generated by an external cavity laser (ECL) at 1550.12 nm. The half-wave voltage of the MZM is around 5.2 V as can be seen from its transmission curve shown in inset (b). Note that the baud rate of PS-PAM-16 signal is mainly limited by the MZM with a 3 dB bandwidth of ~32 GHz. After 1-km SSMF

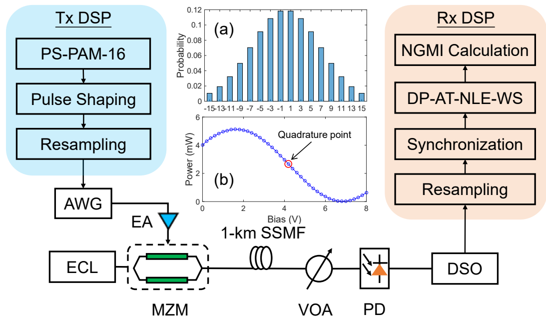

Fig. 1. Experimental setup and DSP block diagram. Insets (a) probability distribution of PS-PAM-16 with 3.7 bit/symbol; (b) measured transmission curve of the used MZM.

transmission, the optical signal is detected by a photo detector (PD). The optical power into the PD is adjusted by a variable optical attenuator (VOA). Here relatively large received optical power (ROP) is required in experiment due to the lack of a trans-impedance amplifier (TIA). Finally, the received electrical signal is captured by digital storage oscilloscope (DSO, Keysight UXR0804A) operating at 256 GSa/s. The off-line DSP includes resampling to 2 samples per symbol, frame synchronization, half-symbol-spaced equalization with 3rd-order DP-AT-NLE-WS, and NGMI calculation. Considering a concatenated FEC with a total code rate of 0.826, the corresponding threshold NGMI for this concatenated FEC is 0.857 [8]. Besides, the weight-sharing kernels are first estimated by recursive least square (RLS) [13] algorithm via the prior-to-signal training sequence and then clustered by *k*-means clustering algorithm [12], which are unchanged in equalization process for data transmission.

We first optimize the three parameters including memory length, pruning factor and the number of cluster centroids of the NLEs in a C-band IM/DD short-reach transmission system over 1-km SSMF at a ROP of 6 dBm. The 100-GBaud PS-PAM-16 signal with 3.7-bit/symbol (net [3.7-(1-0.826)×$\log_2(16)$]×100 = 300.4 Gbit/s) is chosen for parameter optimization. Fig. 2(a) shows the measured NGMI as a function of the linear memory length N_1 for linear equalizer (LE). One can see that the NGMI firstly increases with the increase of the memory length N_1. When the memory length N_1 is larger than 200, the NGMI improvement becomes negligible. The NGMI still cannot reach the SD-FEC threshold of 0.857 using LE even when the memory length N_1 reaches up to 400. Therefore, N_1 = 200 is chosen for all NLEs.

The measured NGMI versus the nonlinear memory length N_{nl} at different pruning factors Q for the 3rd-order DP-VNLE and DP-AT-NLE is shown in Fig. 2(b). For consistency, 2nd- and 3rd-order nonlinear memory lengths N_2 and N_3 are set to be the same as N_{nl}. It is observed that the NGMI is significantly improved over the SD-FEC threshold of 0.857 after equalization with 3rd-order DP-VNLE or DP-AT-NLE. Meanwhile, a larger nonlinear memory length N_{nl} or a larger pruning factor Q can help to improve the NGMI before the performance saturation at N_{nl} = 34 and Q = 4. Based on the pre-validated NGMI results, $N_2 = N_3$ = 34 and Q = 4 are set for all NLEs in the following experiment.

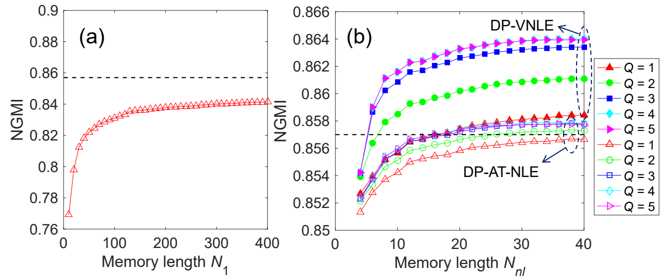

Fig. 2. (a) Measured NGMI versus memory length N_1 for LE; (b) measured NGMI versus nonlinear memory length N_{nl} at different pruning factors Q for DP-VNLE and DP-AT-NLE with N_1 = 200.

The number of cluster centroids (i.e., new kernels) and their values of DP-AT-NLE-WS are required to be optimized based on the kernels of DP-AT-NLE with N_1 = 200, $N_2 = N_3$ = 34, and Q = 4. The measured NGMI versus the number of clusters for 3rd-order DP-AT-NLE-WS after 1-km SSMF transmission at a ROP of 6 dBm is shown in Fig. 3(a). For comparison, the results of 3rd-order DP-VNLE-WS, 2nd-order DP-VNLE-WS and DP-AT-NLE-WS are included. It is seen that: (1) The NGMI increases with the increase of the number of cluster centroids (i.e., kernels) for both DP-VNLE-WS and DP-AT-NLE-WS. (2) The equalization performance of DP-VNLE-WS is slightly better than that of DP-AT-NLE-WS, at the cost of higher computational complexity, as can be seen in Fig. 3(b). (3) The NGMIs of both the 2nd-order DP-VNLE-WS and DP-AT-NLE-WS cannot approach the SD-FEC threshold of 0.857 due to residual 3rd-order nonlinear distortion. (4) To reach the NGMI threshold of 0.857, the required number of clusters for 3rd-order DP-VNLE-WS and DP-AT-NLE-WS are 80 and 114 at least, respectively.

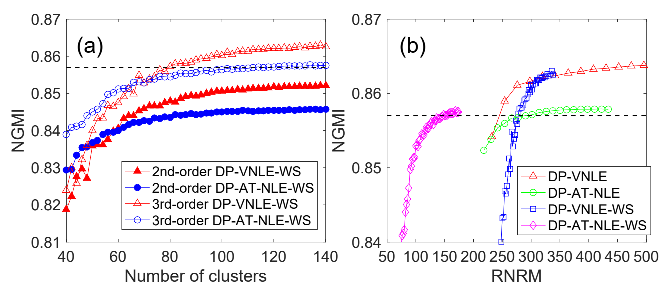

Fig. 3. (a) Measured NGMI versus the number of clusters for different NLEs; (b) measured NGMI versus RNRM for different NLEs.

We then compare the equalization performance and complexity among abovementioned 3rd-order NLEs. Based on the complexity calculation presented in Table 1, the RNRMs of the proposed 3rd-order DP-AT-NLE-WS and DP-VNLE-WS are altered by varying the number of cluster centroids (i.e., new kernels) at N_1 = 200, $N_2 = N_3$ = 34, and Q = 4, while the RNRM curves of the 3rd-order DP-VNLE and DP-AT-NLE are obtained by varying the nonlinear memory length N_{nl} at N_1 = 200 and Q = 4. Fig. 3(b) depicts the measured NGMI versus RNRM for different 3rd-order NLEs.

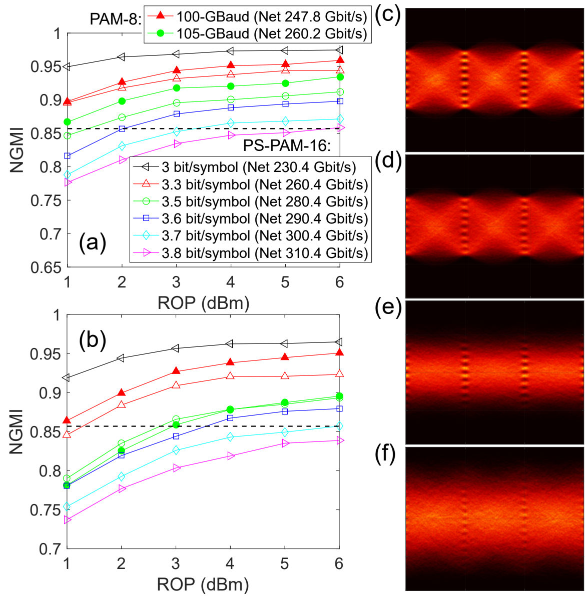

Fig. 4. Measured NGMI versus ROP of 100-Gbaud PAM-8 and 100-Gbaud PS-PAM-16 with different entropies after (a) BtB and (b) 1-km SSMF transmissions; recovered eye diagrams for (c) 100-GBaud PAM-8, (d) 105-GBaud PAM-8, and 100-Gbaud PS-PAM-16 with (e) 3.3 bit/symbol and (f) 3.7 bit/symbol after 1-km SSMF transmission at a ROP of 6 dBm.

Thanks to the absolute operation instead of the multiplication operation and the reduction of kernel redundancy, the proposed 3rd-order DP-AT-NLE-WS only needs 148 real-valued multiplications for net-300.4-Gbit/s transmission at the NGMI threshold of 0.857, which lowers the RNRM by 41.7%, 49%, and 46.8% compared with 254, 290 and 278 real-valued multiplications of the 3rd-order DP-VNLE, DP-AT-NLE, and DP-VNLE-WS, respectively. Moreover, the proposed 3rd-order DP-AT-NLE-WS not only achieves better NGMI performance but also saves 26% real-valued multiplications, in comparison with LE at $N_1 = 200$.

Finally, we evaluate the system performance based on the proposed nonlinearity-aware PS-PAM-16 transmission scheme using 3rd-order DP-AT-NLE-WS with only 114 kernels. Figures 4(a) and 4(b) show the measured NGMI versus ROP for 100-GBaud PS-PAM-16 signal transmissions over back-to-back (BtB) and 1-km SSMF, respectively. The transmission results of PAM-8 signals at 100-GBaud and 105-GBaud are also depicted in Figs. 4(a) and 4(b). Besides, the corresponding eye diagrams for 100-GBaud PAM-8, 105-GBaud PAM-8 and 100-Gbaud PS-PAM-16 with 3.3 bit/symbol and 3.7 bit/symbol after 1-km SSMF transmission are presented in Figs. 4(c) to 4(f), respectively. It can be concluded that: (1) The highest net data rates for PS-PAM-16 signal are 310.4 Gbit/s and 300.4 Gbit/s for BtB and 1-km SSMF transmissions, respectively. (2) Due to the fiber chromatic dispersion (CD) induced power fading, the NGMI performance of 1-km transmission is slightly degraded compared to BtB case. (3) Owing to the sharp pulse shaping and the severe system bandwidth constraint, significant shaping gain can be achieved by 3-bit/symbol PS-PAM-16 in terms of NGMI performance, in comparison with PAM-8 at the same symbol rate [14]. (4) At net 260-Gbit/s, the PS-PAM-16 outperforms the PAM-8 signal due to the severer bandwidth limitation of higher symbol rate transmission. (5) Compared with 100 (105)-GBaud PAM-8 signal at net 247.8 (260.2) Gbit/s, the 100-GBaud PS-PAM-16 can support beyond net 300 Gbit/s after 1-km SSMF transmission at a ROP of 6 dBm, resulting in 21.2% (15.5%) improvement of system capacity.

In conclusion, we have proposed and experimentally demonstrated a nonlinearity-aware signal transmission scheme based on a low-complexity 3rd-order DP-AT-NLE-WS and rate-adaptable PS-PAM-16 signal for net-300-Gbit/s/λ short-reach optical interconnects in C band. By applying absolute operation and weight sharing, the proposed 3rd-order DP-AT-NLE-WS saves > 40% real-valued multiplications compared to the 3rd-order DP-VNLE, DP-AT-NLE and DP-VNLE-WS, with the achieved NGMI larger than the SD-FEC threshold of 0.857. Employing a commercial 32-GHz MZM and a single DAC, C-band single-lane PS-PAM-16 signal transmission using low-complexity DP-AT-NLE-WS over 1-km SSMF have been realized, achieving record 370-Gbit/s line rate and 300.4-Gbit/s net rate. The results show that the proposed nonlinearity-aware PS-PAM-16 transmission scheme is a promising solution for low-complexity high-capacity short-reach optical interconnects beyond net 300 Gbit/s/λ.

Funding. National Key Research and Development Program of China (2018YFB1801701); National Natural Science Foundation of China (62101602, 62035018, 62001415, 62101486); The Hong Kong Government General Research Fund (PolyU 15217620, PolyU 15220120); Natural Science Foundation of Zhejiang Province (LQ21F050013).

Disclosures. The authors declare no conflicts of interest.

Data availability. Data underlying the results presented in this paper are not publicly available at this time but may be obtained from the authors upon reasonable request.

References

1. M. Chagnon, J. Lightwave Technol. **37**, 1779–1797 (2019).
2. X. D. Pang, O. Ozolins, R. Lin, L. Zhang, A. Udalcovs, L. Xue, R. Schatz, U. Westergren, S. Xiao, W. S. Hu, G. Jacobsen, S. Popov, and J. J. Chen, J. Lightwave Technol. **38**, 492–503 (2020).
3. Ethernet Amendment 10: Media Access Control Parameters, Physical Layers, and Management Parameters for 200 Gbps and 400 Gbps Operation, IEEE Standard 802.3bs, 2017.
4. J. Wei, T. Rahman, S. Calabrò, N. Stojanovic, L. Zhang, C. S. Xie, Z. C. Ye, and M. Kuschnerov, Opt. Express **28**, 35240–35250 (2020).
5. T. Wettlin, S. Calabrò, T. Rahman, J. Wei, N. Stojanovic, and S. Pachnicke, "DSP for high-speed short-reach IM/DD systems using PAM," J. Lightw. Technol. **38**. 6771–6778 (2020).
6. J. Zhang, M. Zhu, K. Wang, B. Hua, Y. Cai, M. Lei, Y. Zou, A. Li, W. Xu, J. Wang, X. Liu, Q. Zhou, and J. Yu, *Optical Fiber Communication Conference* 2021, paper Th5F.4.
7. J. Wei, T. Rahman, S. Calabrò, N. Stojanovic, S. B. Hossain, C. Xie, M. Kuschnerov, Z. Ye, *Opto-Electronics and Communications Conference* 2020, 1-3.
8. H. Yamazaki, M. Nakamura, T. Kobayashi, M. Nagatani, H. Wakita, Y. Ogiso, H. Nosaka, T. Hashimoto, and Y. Miyamoto, Opt. Express **27**, 25544–25550 (2019).
9. X. Chen, J. Cho, G. Raybon, D. Che, K. W. Kim, E. Burrows, P. Kharel, C. Reimer, K. Luke, L. He, and M. Zhang, *European Conference on Optical Communication* 2020, 1-4.
10. D. Che and X. Chen, *European Conference on Optical Communication* 2021, 1-4.
11. J. Zhang, Z. Lin, X. Wu, J. Liu, A. P. T. Lau, C. Guo, C. Lu, and S. Yu, Opt. Express **29**, 21891–21901 (2021).
12. X. Wu, J. Zhang, A. P. T. Lau, and C. Lu, Opt. Lett. **47**, 1565–1568 (2022).
13. A. Zaknich, Principles of Adaptive Filters and Self-Learning Systems, (Springer Science & Business Media, 2005).
14. D. Che, J. Cho, and X. Chen, J. Lightw. Technol. **39**, 4997–5007 (2021).

Full references

1. M. Chagnon, "Optical communications for short reach," J. Lightwave Technol. **37**, 1779–1797 (2019).
2. X. D. Pang, O. Ozolins, R. Lin, L. Zhang, A. Udalcovs, L. Xue, R. Schatz, U. Westergren, S. Xiao, W. S. Hu, G. Jacobsen, S. Popov, and J. J. Chen, "200 Gbps/lane IM/DD technologies for short reach optical interconnects," J. Lightwave Technol. **38**, 492–503 (2020).
3. Ethernet Amendment 10: Media Access Control Parameters, Physical Layers, and Management Parameters for 200 Gbps and 400 Gbps Operation, IEEE Standard 802.3bs, 2017.
4. J. Wei, T. Rahman, S. Calabrò, N. Stojanovic, L. Zhang, C. S. Xie, Z. C. Ye, and M. Kuschnerov, "Experimental demonstration of advanced modulation formats for data center networks on 200 Gb/s lane rate IMDD links," Opt. Express **28**, 35240–35250 (2020).
5. T. Wettlin, S. Calabrò, T. Rahman, J. Wei, N. Stojanovic, and S. Pachnicke, "DSP for high-speed short-reach IM/DD systems using PAM," J. Lightw. Technol. **38**. 6771–6778 (2020).
6. J. Zhang, M. Zhu, K. Wang, B. Hua, Y. Cai, M. Lei, Y. Zou, A. Li, W. Xu, J. Wang, X. Liu, Q. Zhou, and J. Yu, "Demonstration of Single-Lane 350-Gb/s PS-PAM-16 in the C-band using single-DAC for Data Center Interconnects," *Optical Fiber Communication Conference* 2021, paper Th5F.4.
7. J. Wei, T. Rahman, S. Calabrò, N. Stojanovic, S. B. Hossain, C. Xie, M. Kuschnerov, Z. Ye, "Transmission of 250 Gb/s Net Rate per Lambda using IMDD PAM-6 and PAM-8," *Opto-Electronics and Communications Conference* 2020, 1-3.
8. H. Yamazaki, M. Nakamura, T. Kobayashi, M. Nagatani, H. Wakita, Y. Ogiso, H. Nosaka, T. Hashimoto, and Y. Miyamoto, "Net-400-Gbps PS-PAM transmission using integrated AMUX-MZM," Opt. Express **27**, 25544–25550 (2019).
9. X. Chen, J. Cho, G. Raybon, D. Che, K. W. Kim, E. Burrows, P. Kharel, C. Reimer, K. Luke, L. He, and M. Zhang, "Single-Wavelength and Single-Photodiode 700 Gb/s Entropy-Loaded PS-256-QAM and 200-GBaud PS-PAM-16 Transmission over 10-km SMF," *European Conference on Optical Communication* 2020, 1-4.
10. D. Che and X. Chen, "Faster-Than-Nyquist Signaling up to 300-GBd PAM-4 and 570-GBd OOK Suitable for Co-Packaged Optics," *European Conference on Optical Communication* 2021, 1-4.
11. J. Zhang, Z. Lin, X. Wu, J. Liu, A. P. T. Lau, C. Guo, C. Lu, and S. Yu, "Low-complexity sparse absolute-term based nonlinear equalizer for C-band IM/DD systems," Opt. Express **29**, 21891–21901 (2021).
12. X. Wu, J. Zhang, A. P. T. Lau, and C. Lu, "Low-complexity absolute-term based nonlinear equalizer with weight sharing for C-band 85-GBaud OOK transmission over a 100-km SSMF," Opt. Lett. **47**, 1565–1568 (2022).
13. A. Zaknich, Principles of Adaptive Filters and Self-Learning Systems, (Springer Science & Business Media, 2005).
14. D. Che, J. Cho, and X. Chen, "Does probabilistic constellation shaping benefit IM-DD systems without optical amplifiers?," J. Lightw. Technol. **39**, 4997–5007 (2021).